

Version 6jan2010:

1. In Equation 12 a typographical error is corrected to use plus sign '+' on second line instead of the incorrect leading minus sign '-'.
2. Figure 3 has been updated to reflect Equation 12 correction (Plot of Bean reflection coefficient has changed).

This article was downloaded by:[University of Washington]

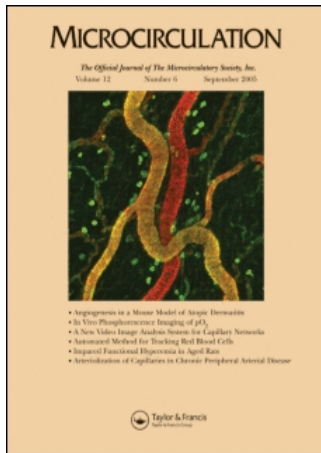
On: 4 September 2007

Access Details: [subscription number 731869354]

Publisher: Informa Healthcare

Informa Ltd Registered in England and Wales Registered Number: 1072954

Registered office: Mortimer House, 37-41 Mortimer Street, London W1T 3JH, UK



Microcirculation

Publication details, including instructions for authors and subscription information:

<http://www.informaworld.com/smpp/title~content=t713723262>

A Practical Extension of Hydrodynamic Theory of Porous Transport for Hydrophilic Solutes

James B. Bassingthwaight^a

^a Department of Bioengineering, University of Washington, Seattle, Washington, USA

Online Publication Date: 01 March 2006

To cite this Article: Bassingthwaight, James B. (2006) 'A Practical Extension of Hydrodynamic Theory of Porous Transport for Hydrophilic Solutes', *Microcirculation*, 13:2, 111 - 118

To link to this article: DOI: 10.1080/10739680500466384

URL: <http://dx.doi.org/10.1080/10739680500466384>

PLEASE SCROLL DOWN FOR ARTICLE

Full terms and conditions of use: <http://www.informaworld.com/terms-and-conditions-of-access.pdf>

This article maybe used for research, teaching and private study purposes. Any substantial or systematic reproduction, re-distribution, re-selling, loan or sub-licensing, systematic supply or distribution in any form to anyone is expressly forbidden.

The publisher does not give any warranty express or implied or make any representation that the contents will be complete or accurate or up to date. The accuracy of any instructions, formulae and drug doses should be independently verified with primary sources. The publisher shall not be liable for any loss, actions, claims, proceedings, demand or costs or damages whatsoever or howsoever caused arising directly or indirectly in connection with or arising out of the use of this material.

© Taylor and Francis 2007

A Practical Extension of Hydrodynamic Theory of Porous Transport for Hydrophilic Solutes

JAMES B. BASSINGTHWAIGHTE

University of Washington, Department of Bioengineering, Seattle, Washington, USA

ABSTRACT

Objective: The equations for transport of hydrophilic solutes through aqueous pores provide a fundamental basis for examining capillary–tissue exchange and water and solute flux through transmembrane channels, but the theory remains incomplete for ratios, α , of sphere diameters to pore diameters greater than 0.4. Values for permeabilities, P , and reflection coefficients, σ , from Lewellen (18), working with Lightfoot et al. (19), at $\alpha = 0.5$ and 0.95, were combined with earlier values for $\alpha < 0.4$, and the physically required values at $\alpha = 1.0$, to provide accurate expressions over the whole range of $0 < \alpha < 1$.

Methods: The “data” were the long-accepted theory for $\alpha < 0.2$ and the computational results from Lewellen and Lightfoot et al. on hard spheres (of 5 different α 's) moving by convection and diffusion through a tight cylindrical pore, accounting for molecular exclusion, viscous forces, pressure drop, torque and rotation of spheres off the center line (averaging across all accessible radial positions), and the asymptotic values at $\alpha = 1.0$. Coefficients for frictional hindrance to diffusion, $F(\alpha)$, and drag, $G(\alpha)$, and functions for $\sigma(\alpha)$ and $P(\alpha)$, were represented by power law functions and the parameters optimized to give best fits to the combined “data.”

Results: The reflection coefficient $\sigma = \{1 - [1 - (1 - \phi)^2]G'(\alpha)\} + 2\alpha^2\phi F'(\alpha)$, and the relative permeability $P/P_{\max} = \phi F'(\alpha)[1 + 9\alpha^{5.5} \cdot (1.0 - \alpha^5)^{0.02}]$, where ϕ is the partition coefficient or volume fraction of the pore available to solute. The new expression for the diffusive hindrance is $F'(\alpha) = (1 - \alpha^2)^{3/2}\phi/[1 + 0.2 \cdot \alpha^2 \cdot (1 - \alpha^2)^{16}]$, and for the drag factor is $G'(\alpha) = (1 - 2\alpha^2/3 - 0.20217\alpha^5)/(1 - 0.75851\alpha^5) - 0.0431[1 - (1 - \alpha^{10})]$. All of these converge monotonically to the correct limits at $\alpha = 1$.

Conclusions: These are the first expressions providing hydrodynamically based estimates of $\sigma(\alpha)$ and $P(\alpha)$ over $0 < \alpha < 1$. They should be accurate to within 1–2%.

Microcirculation (2006) **13**, 111–118. doi:10.1080/10739680500466384

KEY WORDS: capillary permeability, convection, diffusion, hydrodynamic equations, interstitial matrix, membrane transport, molecular exclusion, osmotic water and solute fluxes, particle flow in fluids, porous transport model, steric hindrance

Pappenheimer et al. (21) used Poiseuille's law for flow through cylindrical tubes to predict capillary hydraulic conductivity as if there were a set of uniform cylindrical pores traversing the capillary endothelium. When pore dimensions approach molec-

ular dimensions any macroscale continuum description might be expected to fail. One reason is that at small scales, any structuring of water molecules might be expected to raise the effective viscosity. Levitt (16), however, using molecular dynamic calculations, found the Poiseuille flow expressions to work surprisingly well for the transport of water through 3.2-Å-radius pores, even when the water molecules were modeled as hard spheres of 1-Å radius. Other experimental methods used to determine the pore radius include measuring the pressure necessary to balance the surface tension of fluid in the pores, finding the radius of the largest solute that penetrates the membrane, and examining the pore dimensions revealed by electron microscopy. These issues are well explained by Curry in a masterful review (8).

This work was supported by NIH grant EB01973 and HL073598. The author is highly appreciative of the editorial assistance of James E. Lawson, and the figure preparation assistance of Kay A. Sterner.

Address correspondence to James B. Bassingthwaighte, MD, PhD, University of Washington, Department of Bioengineering, Box 357962, Seattle, WA 98195-7962, USA. E-mail: jbb@bioeng.washington.edu

Received 29 August 2005; accepted 22 September 2005.

The hydraulic conductivity, L_p , for flow of a Newtonian fluid through a population of uniform cylindrical pores, following Poiseuille's relationship at low Reynold's numbers without turbulence, is

$$L_p = \frac{A_p r_p^2}{8\eta A_m \Delta x} = \frac{A_p}{A_m} \frac{r_p^2}{8\eta \Delta x} = \frac{N_p}{A_m} \frac{\pi r_p^4}{8\eta \Delta x} \quad (1)$$

where A_p (cm^2), is the total pore area available for water transport and equals the number of pores N_p times the cross-sectional area of the pore for water transport; A_m is the total capillary surface area; η is the solvent viscosity; poise (p) = $\text{dyn}/\text{cm}^2 = \text{g s}^{-1} \text{cm}^{-1}$, r_p is the pore radius (cm), and Δx is the pore length (cm). L_p (cm s^{-1}) (mmHg^{-1}), or ($\text{cm}^2 \text{g}^{-1} \text{s}$), can be interpreted in terms of two characteristic pore parameters, r_p , and the lumped parameter $A_p/A_m \Delta x$, the fractional pore area per path length. This defines the filtration coefficient, $k_F = L_p$. For a long, parallel-walled slit the equivalent equation is

$$L_p = \frac{A_p w^2}{12\eta A_m \Delta x} \quad (2)$$

where the pore radius is replaced by the slit width, w . Pappenheimer et al. (21) used these equations to calculate the hydraulic conductivity for capillaries in the hind limbs of cats as equivalent to uniform cylindrical pores with radii of 3 nm or slits of 3.7-nm width.

For solute traversing such pores the process of molecular diffusion is slowed when the mobility of the solute decreases, so a solute in a pore must have a diffusion coefficient, D_p , less than that in free solution. This restriction becomes more significant as the solute's molecular dimensions approach those of the pore. Additionally, solute may be sterically restricted from entering some regions of the pore (Figure 1). A spherical solute cannot occupy a position in a pore

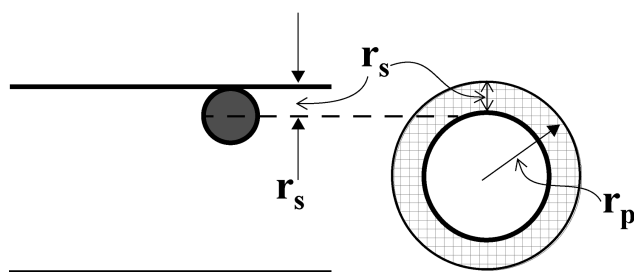


Figure 1. A spherical solute with radius r_s in a cylindrical pore is excluded from the cross-hatched region within r_s of the cylinder wall.

within one solute radius from the pore's edge, so for a cylindrical pore the solute partition coefficient can be calculated from

$$\phi = \frac{\pi(r_p - r_s)^2}{\pi r_p^2} = (1 - \alpha)^2 \quad (3)$$

where $\alpha = r_s/r_p$, the ratio of solute radius, r_s , to pore radius, r_p . The solute's partition coefficient, ϕ , is the ratio of the area available to the solute to the total pore surface area, and is a standard partition coefficient equal to the equilibrium ratio of the solute concentration within the pore to that outside, in the surrounding solution. With respect to diffusional mobility, the exclusion phenomena represents only the limitation to the volume of water inside the pore available for solute diffusion, and does not account for the frictional hindrance that the wall exerts on the particle through the viscosity of the fluid. The permeability coefficient (cm s^{-1}) is related to these parameters by

$$P = \frac{A_p}{A_m} \phi \frac{D_p}{\Delta x} \quad (4)$$

where D_p is the effective diffusion coefficient within the pore. The ratio of D_p to D_{fr} , the free diffusion coefficient in the external solution, is defined by a frictional hindrance factor $F(\alpha)$, such that $0 < F(\alpha) < 1$, and giving P

$$P = \frac{A_p}{A_m} (1 - \alpha)^2 F(\alpha) \frac{D_{fr}}{\Delta x} \quad (5)$$

Defining a maximum permeability for a solute for which there is no hindrance, $\alpha = 0$ and $F(\alpha) = 1$, then P relative to an unhindered permeability is

$$\frac{P}{P_{\max}} = \phi F(\alpha) \quad (6)$$

$F(\alpha)$ is a factor ($0 < F < 1$) that defines the reduction in diffusion due to hindrance. It is given by Curry's Eq. 5.17 (8), which is the same as that given by Faxén's (10) paper,

$$F(\alpha) = 1 - 2.10444\alpha + 2.08877\alpha^3 - 0.94813\alpha^5 - 1.372\alpha^6 + 3.87\alpha^8 - 4.19\alpha^9 \quad (7)$$

and is shown by the lower black dashed line in Figure 2. It is intended, via Eq. 6, to characterize the ratio of the diffusion coefficient inside the pore to that outside, D_p/D_{fr} (2,3,8,10). Beck and Schultz (4) obtained permeability data on 7 solutes with radii

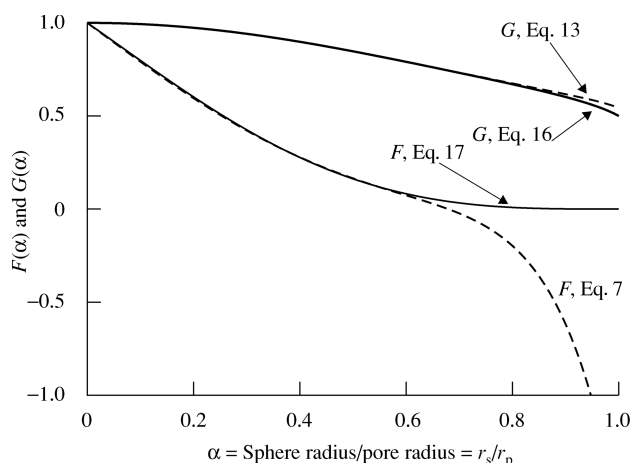


Figure 2. Hydrodynamic functions $F(\alpha)$ and $G(\alpha)$ for cylindrical pores. In the classical formulations given by the black dashed lines, $F(\alpha)$ is given by Eq. 7 and $G(\alpha)$ by Eq. 13. Both are incorrect at high values of α ; $F(\alpha)$ should not go negative but should diminish monotonically to zero; $G(\alpha)$ should go smoothly to 0.5, which is the average velocity of the fluid and particle when the sphere fills the cylinder diameter and is half the centerline velocity of parabolic flow in the limit as α goes to zero. The new (corrected) formulae given in Eqs. 16 and 17 for $F'(\alpha)$ and $G'(\alpha)$, the red and blue lines, converge to the required limits.

from 2.64 to 8.47 Å through mica microporous membranes of known pore sizes from 45 to 300 Å equivalent diameter, and using only the first three terms of Eq. 7 demonstrated its accuracy for small α . However, it fails at large α , as is evident from its negative portion, and must for physical reasons converge monotonically to zero at $\alpha = 1$.

For a parallel-walled slit, the equation for permeability (7) is

$$P = \frac{A_p}{A_m} (1 - \alpha) F_{\text{slit}}(\alpha) \frac{D_{\text{fr}}}{\Delta x} \quad (8)$$

In this context, α becomes the ratio of solute radius to one-half the slit width, $\alpha = r_s/(w/2)$, with

$$F_{\text{slit}}(\alpha) = 1.0 - 1.004\alpha + 0.418\alpha^3 + 2.10\alpha^4 - 0.1696\alpha^5 \quad (9)$$

The context for these equations is to describe simultaneous water and solute fluxes across porous membranes, and therefore one needs to define the solute reflection coefficient as well as its permeability. From the Kedem and Katchalsky (13) or the Patlak (22) solute flux equation, the reflection coefficient can be

defined as

$$\sigma = 1 - \left(\frac{J_s}{J_v C} \right)_{\Delta c=0} \quad (10)$$

Since J_s is the actual solute flow and C the external solute concentration, $J_v C$ is the total amount of solute flux that would occur if there were no hindrances to entry or diffusion. The ratio $J_s/J_v C = \phi$ would be a good descriptor if solute were transported at the mean convective velocity of the fluid, so Eq. 10 might be rewritten as the approximation

$$\sigma = 1 - \phi = 1 - (1 - \alpha)^2 \quad (11)$$

This derivation of the solute reflection coefficient ignores the frictional interaction of solute and water within the pore, and the nonuniform solvent velocity within the pore. Early estimates of solute reflection coefficients were made by Ferry (11), who accounted for the presence of a parabolic velocity profile while calculating a filtration coefficient for an artificial membrane by assuming that the solute in the pore moved at the local water velocity. Renkin (23) predicted the reflection coefficient for a spherical solute traveling through a cylindrical pore and attempted to include the effects of the frictional interaction with the water. Bean (3), first realized that the term $F(\alpha)$ should be replaced by the hydrodynamic function $G(\alpha)$, which accounts for the difference between solute velocity and water velocity (Figure 2). Additionally, Bean accounted for the effects of pressure on the solute velocity where the solute was positioned on the centerline and derived the expression for the cylindrical pore:

$$\sigma = 1 - [2(1 - \alpha)^2 - (1 - \alpha)^4]G(\alpha) + 16/9\alpha^2(1 - \alpha)^2F(\alpha) \quad (12)$$

These are the same pore equations that Curry (8) used to determine L_p , P , and σ , where $G(\alpha)$ is a hydraulic factor accounting for the difference in solute and water velocities, and $0.5 < G < 1$. Using the equation from Curry's Eq. 5.51 (8), $G(\alpha)$ is

$$G(\alpha) = \frac{1 - 2\alpha^2/3 - 0.20217\alpha^5}{1 - 0.75851\alpha^5} \quad (13)$$

which is for a solute on the axis (centerline) of the cylinder and is accurate for $\alpha < 0.6$ and overestimates G modestly for larger α 's (smaller G 's) as shown in Figure 2.

Other investigators, including Anderson and Quinn (1) and Curry (7), using more complex theories, have

developed numerically similar or identical expressions. The equivalent expression derived for a rectangular slit is (7)

$$\sigma_{\text{slit}} = \frac{2\alpha^2}{3}(1-\alpha)F_{\text{slit}}(\alpha) + \frac{3}{2}(1-\alpha)\left(\frac{2}{3} + \frac{2}{3}\alpha - \frac{7}{12}\alpha^2\right) \quad (14)$$

The $F_{\text{slit}}(\alpha)$ expression also fails at high α , demonstrating that the hydrodynamic theory is incomplete.

To improve on this situation, Lightfoot et al. (19), and Lewellen (18) tackled the problem from the point of view of low Reynold's number hydrodynamics, building upon the work of Bungay and Brenner (5), whose development was good for $\alpha < 0.25$. The Lightfoot 1976 study defined values of the reflection coefficient σ for low $\alpha < 0.25$, while Lewellen's thesis (18) provided values of σ for α at a middle and a high value, an immense computer calculation taking into account the details of the processes, torque, radial position, molecular eccentricity, and density profiles for the solute within the tube.

For this study, the results of the computations of Lightfoot et al. and of Lewellen are used to formulate expressions for $F(\alpha)$, $G(\alpha)$, σ , and P . The approach is to consider these sparse calculations as "data," which are to be fitted with continuum expressions for $F(\alpha)$ and $G(\alpha)$, and from which one derives the desired continuum expressions for σ and P . The result is that for the first time we have available expressions that cover the full range of $\alpha = r_s/r_p$, and that provide full hydrodynamic calculation fairly precisely.

METHODS

The results from Lightfoot et al. (19), and Lewellen (18) are provided in Table 1. The results were based on the full hydrodynamic treatment for solute convective and diffusive velocities within the pore, making the calculations for centerline position and for all the off-center positions within the accessible region of

the pore. An arbitrary decision had to be made about the probability of occurrence of each radial position, since no observations are available for molecules in pores, and the decision was to assume uniformity of solute density across the nonexcluded region at each α . (Since it is known that red cells migrate to some extent toward the centerline (24,25), presumably because they have flexibility, it opens the question of whether or not hard spheres might behave similarly, in which case the assumption of uniform cross-section density would have to be reevaluated.)

A way of viewing porous transport in general is to consider that the steric hindrance and the geometry of the pathway through which both solute and water move define four things: (1) the water conductance per channel; (2) the solute permeability per channel; (3) the solute reflection coefficient; (4) solute-solvent interaction, solvent drag. The reflection coefficient is independent of the numbers of channels, but the total water conductance is the single-channel conductance times the number of channels, just as the total permeability is the product of the single-channel permeability times the number of channels.

Based on these premises, the strategy was to find continuum expressions for $F(\alpha)$ and $G(\alpha)$ that fit the historically well-worked formulae at small α and fit the "data" of Table 1 and finally, have the correct convergences for $F(\alpha)$ and $G(\alpha)$ at $\alpha = 1$. The fitting of the "data" means fitting the reflection coefficient and permeability with expressions continuous over $0 < \alpha < 1$.

New equations were developed to try to simplify the power series representation of $F(\alpha)$ and $G(\alpha)$ while forcing them to terminate properly with values of zero and 0.5, respectively, at $\alpha = 1$. The previous power series expressions given above were considered to be correct at low α , and were therefore used as a basis for modifying the expressions.

Scalar expressions were used to modify $F(\alpha)$ and $G(\alpha)$ smoothly over parts of the range of α . A generic expression, having a great flexibility of shape over

Table 1. Estimates of σ and P for hard spheres in a cylindrical pore

$\alpha = r_s/r_{\text{pore}}$	σ	P/P_{max}	Ref	σ , Eq. 18	P/P_{max} , Eq. 19
0.05	0.019	—	Lightfoot et al. (19)	0.015	0.811
0.13	0.083	—	Lightfoot et al. (19)	0.088	0.557
0.23	0.224	—	Lightfoot et al. (19)	0.228	0.323
0.5	0.665	0.047	Lewellen (18)	0.650	0.048
0.95	0.997	1.48×10^{-6}	Lewellen (18)	0.997	1.44×10^{-6}

$0 < \alpha < 1$, is the scalar $S(\alpha)$:

$$S(\alpha) = 1 + k_1 \alpha^{k_2} (k_3 - \alpha^{k_4})^{k_5} \quad (15)$$

where k_1 is an overall scalar for the function, the exponents k_2 and k_4 to α provide amplification factors, and the exponent k_5 provides for positioning along the α axis.

By adjusting the parameters of $S(\alpha)$ by optimization, the curves for $P(\alpha)$ and $\sigma(\alpha)$ minimize the squared differences between the curves for P and σ and the “data” of Table 1 at the given values of α . Decreasing k_2 scales the peak up and toward smaller α ; increasing k_2 reduces the peak and shifts it to higher α . The value of k_3 is normally kept at 1.0, unless a nonzero value is desired at $\alpha = 1.0$. Decreasing k_4 lowers the peak and shifts it to the left, while raising it shifts the peak up and to the right. Decreasing k_5 raises the peak and moves it toward higher α while increasing k_5 lowers the peak and shifts it to smaller α . Scalars of this general form were used to modify the curves for $F(\alpha)$ and $G(\alpha)$ to give good fits of σ and P to the “data.”

RESULTS

The calculated “data” of Lightfoot et al. (19) and of Lewellen (18) for σ and P are in columns 2 and 3 of Table 1. These specify the targets for the optimization.

The new equations are $F'(\alpha)$ and $G'(\alpha)$ to replace the old $F(\alpha)$ and $G(\alpha)$:

$$F'(\alpha) = \frac{(1 - \alpha^2)^{3/2} \phi}{1 + 0.2\alpha^2(1 - \alpha^2)^{16}} \quad (16)$$

$$G'(\alpha) = \frac{1 - 2\alpha^2/3 - 0.20217\alpha^5}{1 - 0.75851\alpha^5 - 0.0431[1 - (1 - \alpha^{10})]} \quad (17)$$

where ϕ is the partition coefficient or volume fraction of the pore available to solute. $F'(\alpha)$ is almost entirely dominated by the numerator. The numerator is virtually identical *numerically* to the earlier expression in Eq. 7 for $\alpha < 0.6$, although it is simpler, is close to the “data” at $\alpha = 0.5$ and 0.95 , and is exact at $\alpha = 1.0$. The denominator could be set at 1.0 except for the need for fine tuning to obtain the correct $F'(\alpha)$ for $\alpha < 0.5$, the largest value taken by the denominator is 1.0044 at $\alpha < 0.24$, a change from the numerator alone of 0.4%.

The $G'(\alpha)$ was taken to be the same as in Eq. 13 except for the additional second term, which forces

the values of $G'(\alpha)$ to 0.5 at $\alpha = 1$, a correction relevant only to the largest spheres. The reason that the old equations for $F(\alpha)$ and $G(\alpha)$ remained incomplete, as shown by the dashed lines in Figure 2, for so many years is that in calculating the reflection coefficient, σ , and the permeability, P , for large spheres the values of $F'(\alpha)$ and $G'(\alpha)$ are almost irrelevant since the values of ϕ dominate the estimate at large α .

New equations for the reflection coefficient, σ , and the permeability, P , are

$$\sigma = 1 - [1 - (1 - \phi)^2]G'(\alpha) + 2\alpha^2\phi F'(\alpha) \quad (18)$$

and

$$\frac{P}{P_{\max}} = \phi F'(\alpha)[1 + 9\alpha^{5.5}(1 - \alpha^5)^{0.02}] \quad (19)$$

There are no arbitrary correction terms in Eq. 18. The parenthetical correction term in Eq. 19 has no effect until $\alpha > 0.4$, and then rises from 1 to 8. As was true of the polynomials classically used in Eqs. 7 and 13, the calculation of P has little sensitivity to the final value of the scalar since both ϕ and $F'(\alpha)$ converge to zero.

Figure 3 shows the curves for σ and P for the old and new formulations. In Table 1, the two rightmost columns, are the estimates of σ and P using the new equations, for comparison with the “data” in columns 2 and 3. The curve for σ matches the data points of Lightfoot et al. (19), matches Eq. 5.49b of Curry (8), matches the “data” of Lewellen (18), and asymptotes smoothly to zero.

Figure 4 provides an example of data integration using the new expression for σ . A detailed model for the simultaneous exchange of water and solutes across the capillary wall was developed by Kellen and Bassingthwaighte (14), accounting for water flux across endothelial cells as well as through interendothelial clefts. The reflection coefficients estimated for seven solutes in osmotic transient experiments on isolated Krebs-Henselt-perfused rabbit hearts by Kellen and Bassingthwaighte (15) are fitted by Eq. 18 to provide an estimate of an equivalent pore radius of 7.9 nm.

DISCUSSION

This analysis extends the prior studies on the hydrodynamics of convection and diffusion of hard spheres within a right cylindrical pore by providing simple

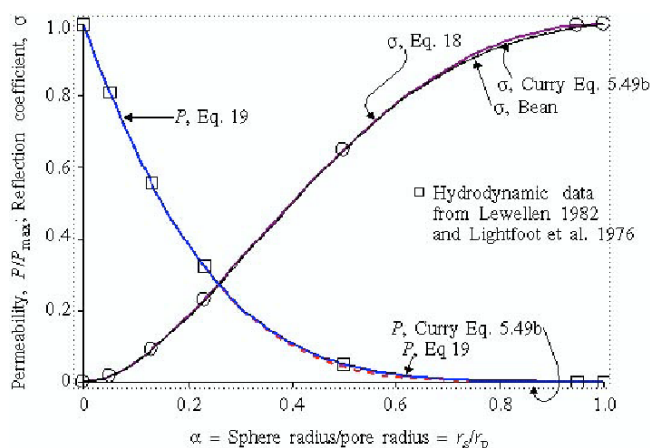


Figure 3. Permeability, P/P_{\max} , and reflection coefficients, σ . The solid lines give the results of this study, using the new formulae for $F'(\alpha)$ and $G'(\alpha)$ for σ in Eq. 18 and for P in Eq. 19. Bean's (3) equation for σ is the dashed line. Curry's (8) Eq. 5.49b for σ is given by the dotted line, which is almost identical to Eq. 18 (though Curry's and our equations for $F'(\alpha)$ are quite different) until it emerges to take a lower course for values of $\alpha > 0.7$. Likewise, the curves for Curry's and our permeabilities are similar at $\alpha < 0.4$. At high α Curry's P is too low and actually a little negative due to the error in $F(\alpha)$ going negative at large α . The new $F'(\alpha)$ converges monotonically to zero at large α , as shown in Figure 2, and gives values of P matching the estimate at $\alpha = 0.95$ by Lewellen (18).

numerical calculations for P and σ that cover the full range of $0 < \alpha < 1$. The descriptive fitting function is an essential feature of this field, in the style of its early workers like Faxén in providing a power series approximation to describe the curve.

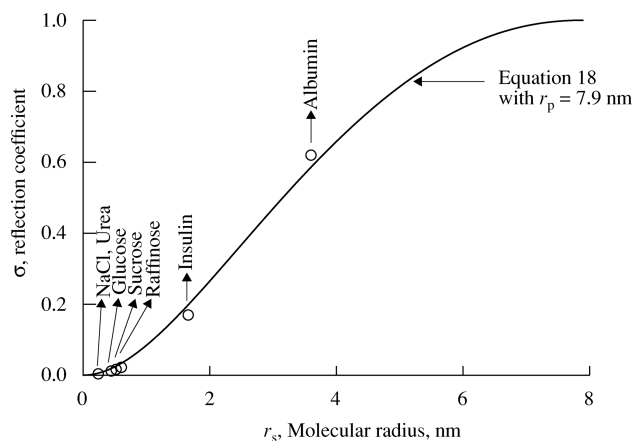


Figure 4. Reflection Coefficient, σ , for hydrophilic solutes in capillaries of perfused rabbit hearts as a function of molecular radius, using single pore analysis, Eq. 18. (Data from Kellen and Bassingthwaite (15) (Table 3.)

While this is a seeming success, the particular parameters for the equations above are certainly not unique, and other sets will be found to be as good. The Bean calculations for σ contain errors, described by Lewellen. There are errors also in the Curry calculation, but these almost cancel, again according to a detailed appraisal by Lewellen. The Curry equation, his Eq. 5.49b in the 1984 review, is rather close to the hydrodynamic calculations of Lightfoot et al. (19) for low α , and of Lewellen (18) for $\alpha = 0.5$, but is a little low at large α where there were no data for Curry to use. (Here the word "data" is really a misnomer, for it refers to Lightfoot's and Lewellen's computational results.) As Curry and others have pointed out, it has been impossible to obtain data with sufficiently high resolution to test the accuracy of the models.

The early formulae $F(\alpha)$, $G(\alpha)$, P/P_{\max} , and σ were polynomial expressions fitted to hydrodynamic calculations for chosen values of α , and accounted for steric exclusion. The introduction of the frictional term, $F(\alpha)$, and $G(\alpha)$, greatly improved the estimates, even though they were based on the "centerline approximation," the assumption that the diffusion and drag found for a sphere at the axis of the cylinder was applicable to eccentrically positioned spheres. The calculations of Bungay and Brenner, of Lightfoot et al., and of Lewellen, took into account the full hydrodynamics, that is, the steric exclusion, the hindrances to diffusion, the drag, and the pressure drop across the sphere, and the torque and rotation produced by viscous interactions with the wall when the sphere is eccentrically positioned. These authors all integrated the result over the sterically accessible region of the cylinder, thereby avoiding any assumption based on the "centerline approximation." The consequence of all this effort is that the present study's empirical fits to the "data" integrate all of the detailed hydrodynamic information at various α into a single formulation. Being solidly physically based, these formulations, Eqs. 18 and 19, are presumably the best overall expressions available.

This study is also a provocation to redo the computations of the true hydrodynamics with modern computing methods, over the whole range of $0 < \alpha < 1$. Then the data points could be refitted using a strategy such as is used here, to end up with yet more accurate formulae. Further, all of our expressions assume no interactions between solute particles, so these expressions must fail at high concentrations of larger solutes, which cannot pass each other ($\alpha = 0.5$) and which cause hydrodynamic interactions at a distance [6].

Applications using reflection coefficients and permeabilities in combination are extensive in the literature using the irreversible thermodynamic approach of Kedem and Katchalsky (13), with much exploration of the nature of porous transport through the capillary membrane of isolated capillaries and capillaries in intact organs. Levitt (17) derived the Onsager reciprocal relationship that was fundamental to irreversible thermodynamics from hydrodynamic calculations, a result that extended confidence in such approaches. The reason for this strenuous effort has been to understand substrate exchanges between blood and tissue, and to explain water and protein transport between blood and lymph.

The equations for P and σ are useful in designing experiments to characterize membranes. Provided that measurement of the fluxes of water and of a series of solutes of differing molecular size is possible, and given that some of the molecular sizes approach the channel size, so the degree of hindrance is measurable, characterization is straightforward but not simple. A set of solutes for which $P/(D/\Delta x)$ are different must be chosen, that is, a set of solutes with sizes that cause differing degrees of hindrance. One of these solutes should have a reflection coefficient of 1.0, so L_p can be estimated from osmotic water flux; the estimate should be verified by comparison with the estimate of L_p from a pressure-driven flux. With two or more other solutes of smaller size, and the estimates of P and σ these solutes provide, the pore diameters can be estimated in terms of equivalent cylindrical pores, slits, or other geometry. The numbers of parameters to estimate for the cylinder is four: L_p times S , N_p times S , the diameter, and the pore length, Δx . Permeability is derived from N_p times S , diameter, and pore length. A good exercise in experiment design is to determine the effects of experimental accuracy of the estimates of these parameters.

For a more detailed review of irreversible thermodynamics and its application to coupled solute-solvent transmembrane transport see the texts by Katchalsky and Curran (12) or by Stein (26) and the review in the *Handbook of Physiology* by Curry (8). For porous transport see reviews by Bean (3) and Deen (9). A perspective on applications in microvascular exchange is given by Michel and Curry (20).

REFERENCES

1. Anderson JL, Quinn JA. (1974). Restricted transport in small pores: a model for steric exclusion and hindered particle motion. *Biophys J* 14:130–150.
2. Anderson JL, Malone DM. (1974). Mechanism of osmotic flow in porous membranes. *Biophys J* 14:957–982.
3. Bean CP. (1972). The physics of porous membranes: neutral pores. In: *Membranes: Macroscopic Systems and Models*, (G Einsenman, ed.). Dekker, New York; 1–54.
4. Beck RE, Schultz JS. (1972). Hindrance of solute diffusion within membranes as measured with microporous membranes of known pore geometry. *Biochim Biophys Acta* 255:273–303.
5. Bungay PM, Brenner H. (1973). Pressure drop due to the motion of a sphere near the wall bounding a Poiseuille flow. *J Fluid Mech* 60:81–96.
6. Cui B, Diamant H, Lin B. (2002). Screened hydrodynamic interaction in a narrow channel. *Phys Rev Lett* 89:188302-1–188302-4.
7. Curry FE. (1974). A hydrodynamic description of the osmotic reflection coefficient with application to the pore theory of transcapillary exchange. *Microvasc Res* 8:236–252.
8. Curry FE. (1984). Mechanics and thermodynamics of transcapillary exchange. In: *Handbook of Physiology, Sec. 2: The Cardiovascular System, Vol. 4: Microcirculation*, (EM Renkin and CC Michel, eds). American Physiological Society; Bethesda, MD 309–374.
9. Deen WM. (1987). Hindered transport of large molecules in liquid-filled pores. *AIChE J* 33:1409–1425.
10. Faxén H. (1923). Die bewegung einer starren kugel längs der achse eines mit zäher flüssigkeit gefüllten rohres. *Arkiv För Matematik, Astronomi Och Fysik* 17:1–28.
11. Ferry JD. (1936). Statistical evaluation of sieve constants in ultrafiltration. *J Gen Physiol* 20:95–104.
12. Katchalsky A, Curran PF. (1965). *Nonequilibrium Thermodynamics in Biophysics* Harvard University Press, Cambridge, MA.
13. Kedem O, Katchalsky A. (1958). Thermodynamic analysis of the permeability of biological membranes to non-electrolytes. *Biochim Biophys Acta* 27:229–246.
14. Kellen MR, Bassingthwaighe JB. (2003). An integrative model of coupled water and solute exchange in the heart. *Am J Physiol Heart Circ Physiol* 285:H1303–H1316.
15. Kellen MR, Bassingthwaighe JB. (2003). Transient transcapillary exchange of water driven by osmotic forces in the heart. *Am J Physiol Heart Circ Physiol* 285:H1317–H1331.
16. Levitt DG. (1973). Kinetics of diffusion and convection in 3.2-Å pores. *Biophys J* 13:186–206.
17. Levitt DG. (1975). General continuum analysis of transport through pores, I: proof of Onsager's

- reciprocity postulate for uniform pore. *Biophys J* 15:533–551.
18. Lewellen PC. (1982). *Hydrodynamic Analysis of Microporous Mass Transport*. Ph.D. Thesis, University of Wisconsin–Madison.
 19. Lightfoot EN, Bassingthwaight JB, Grabowski EF. (1976). Hydrodynamic models for diffusion in microporous membranes. *Ann Biomed Eng* 4:78–90.
 20. Michel CC, Curry FE. Microvascular permeability. (1999). *Physiol Rev* 79:703–761.
 21. Pappenheimer JR, Renkin EM, Borrero LM. (1951). Filtration, diffusion and molecular sieving through peripheral capillary membranes: a contribution to the pore theory of capillary permeability. *Am J Physiol* 167:13–46.
 22. Patlak CS, Goldstein DA, Hoffman JF. (1963). The flow of solute and solvent across a two-membrane system. *J Theor Biol* 5:426–442.
 23. Renkin EM. (1954). Filtration, diffusion, and molecular sieving through porous cellulose membranes. *J Gen Physiol* 38:225–243.
 24. Segré G, Silberberg A. (1961). Radial particle displacements in Poiseuille flow of suspensions. *Nature* 189:209–210.
 25. Silberberg A. (1982). The mechanics and thermodynamics of separation flow through porous, molecularly disperse, solid media—the Poiseuille Lecture 1981. *Biorheology* 19:111–127.
 26. Stein WD. (1986). *Transport and Diffusion across Cell Membranes*. Academic Press, Orlando, FL.